SHOCK COMPRESSION OF POROUS TUNGSTEN

K. K. KRUPNIKOV, M. I. BRAZHNIK and V. P. KRUPNIKOVA

Parameters of strong shock waves in tungsten samples of various initial densities were investigated experimentally. Shock adiabats with negative slopes in pressure-density coordinates were found for porous samples at pressures below 0.5×10^6 atm. Bending of the adiabats and a change in the sign of their derivatives were observed with increase of the shock-wave amplitude. This behavior of the adiabats is accounted for by changes in the dependence of the effective Grüneisen constant on the degree of compression and heating due principally to the increase in the electronic specific heat. Expressions are derived relating the partial derivatives $(\partial E/\partial P)_V$ and $(\partial E/\partial v)_P$ with the slopes of two intersecting curves.

INTRODUCTION

SHOCK compression is the principal experimental method used currently to obtain information on the equations of state of metals at high pressures (P), densities ($\rho = 1/v$) and temperatures (T).

Knowledge of only one shock adiabat of a metal for a single initial value of the density gives a single curve in the P—v diagram, and the entropy varies along this curve. Shock adiabats recorded for a series of samples with different initial densities give more data, for a complete region of the P—v diagram can be constructed.[1] In addition, considerably higher temperatures can be studied. The simplest method of obtaining various initial densities is to prepare samples with different porosities $m = \rho_0/\rho_{00} = v_{00}/v_0$ from fine powder; here ρ_0 is the density of solid-metal particles of the sample and ρ_{00} is the mean density of the whole porous sample.

Shock compression of samples of the same substance but of different porosity was first considered theoretically by Ya. B. Zel'dovich and A. S. Kompaneets, who used the equation of state with a constant coefficient $\gamma = v(\partial P/\partial E)_v$. Figure 1 illustrates their results in coordinates of pressure and relative density ($\sigma = \rho/\rho_0$). Shock adiabats of the nonporous material (m = 1) and of samples with various initial porosities (m > 1) all start from the point P = 0, $\sigma = 1$ which represents the initial state of the nonporous material. For a porous body this is the consequence of neglecting the strength of the particles (it is assumed that even a very weak wave is capable of compressing a porous body so that its density becomes ρ_0) and neglecting the energy of dispersion (the initial internal energy per unit mass is assumed to be the
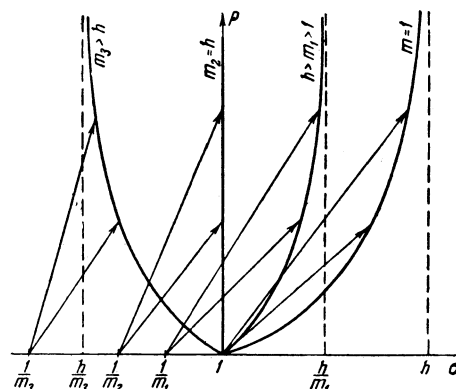

FIG. 1. Compression of porous samples for various values of h/m (h = 1 + 2/γ).

same for the nonporous and porous states).

For equal pressures, the density after shock compression is smaller for a porous body than for a nonporous one, and its value decreases as the initial porosity increases. The physical explanation of this result is as follows (Fig. 2). The path mv_0—v_{por} along which work is done by the shock-compression forces on the porous body is longer than the analogous path v_0—v_{np} for the nonporous body. Since half the work is needed to increase the internal energy, the rise E_T^{por} in the thermal component of the internal energy of a porous body
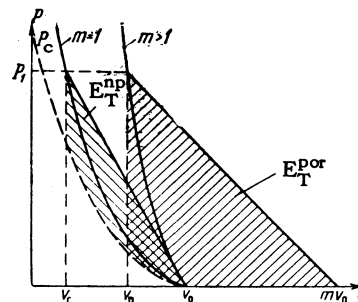

FIG. 2. The P – v diagram for shock compression of porous bodies.

470

is considerably greater than the corresponding quantity (E_T^{np}) for a nonporous body. Thus shock compression of a porous sample is accompanied by greater heating than that of nonporous material. This additional temperature rise increases the thermal component of the pressure, $P_T = P - P_c$, which opposes the compression. Consequently the density of a shock-compressed porous sample is lower than that of a nonporous sample treated in the same way.

For higher values of m the adiabat in the $P-\sigma$ diagram is shifted toward lower values of σ (Fig. 1). Let us denote the limiting compression (as $P \rightarrow \infty$) of a nonporous body by $h = 1 + 2/\gamma$. For the adiabats corresponding to a porosity m_1 in the interval $h > m_1 \geq 1$, the density after shock compression rises with increase of pressure, approaching asymptotically a limiting value $\sigma_{lim} = h/m_1 > 1$. Such adiabats lie in the region $\sigma > 1$ where their slopes $(dP/d\sigma)_H$ are positive.

The role of shock heating is particularly noticeable at porosities $m_3 > h$. Then the adiabats have an unusual inverted form: they lie in the region $\sigma < 1$ and can have derivatives $(dP/d\sigma) < 0$. Whereas a wave of vanishingly small amplitude is capable, as indicated, of compressing a porous sample to the initial density of the nonporous material ($\sigma = 1$), when $m > h$ a wave of finite amplitude cannot produce even such compression. An increase in pressure causes in this case not an increase, but a decrease in the density reached after shock compression, which approaches asymptotically a limiting value $\sigma_{lim} = h/m_3 < 1$. When $m_2 = h$ the adiabat coincides with the ordinate $\sigma \equiv 1$; along this adiabat we have $(dP/d\sigma)_H = \infty$.

Initial experiments with substances with few pores have shown the importance of temperature in shock compression. The results for iron with $m = 1.4$ have been given in [2].

Experiments carried out by the present authors have shown that a very porous body (cotton wool) cannot be shock-compressed to the normal density of the nonporous material. Recently the authors studied shock compressibility of tungsten samples of various initial densities ($m = 1-4$) over a wide range of pressures from several hundred thousand to several million atmospheres. The velocity of sound was measured behind the shock fronts.

EXPERIMENTAL TECHNIQUE

The shock compression parameters D and U (wave and mass velocities) were found using the reflection method described in [3]. A shock wave

of known intensity passed into the sample from a screen, made from a material of known dynamic compressibility. The wave velocity in the sample was found experimentally. Time intervals were recorded with cathode-ray oscillographs.

The tungsten samples had five different initial densities: $m = 1.03$, ≈ 1.8, ≈ 2.15, ≈ 3, and ≈ 4. The density of the nonporous material was taken to be $\rho_0 = 19.35$ g/cm^3. Samples with $m = 1.03$ were drawn from a tungsten bar, and those with larger m were pressed from a powder consisting of $2-3\mu$ particles. The tungsten content of the samples was 99.8% by weight; the principal impurities were molybdenum, iron, phosphorus, copper, and oxygen.

To avoid the effects of lateral disturbances [4] the ratio of the sample diameter to its height was 2 at pressures $\geq 0.9 \times 10^6$ atm; at lower pressures and for samples with larger m, the ratio was 10 or greater. Measurements were carried out over base lengths $3-5$ mm in samples with $m = 1.03$ and over lengths $8-9$ mm in samples with larger m, at pressures $\geq 0.9 \times 10^6$ atm; at lower pressures in samples with large m the wave velocity was successively measured over several base lengths, varying from 1.5 to $5-8$ mm.

The sound velocity was found in shock-compressed samples with $m = 1.8$ using the "lateral relaxation" method.[4] Recording was carried out directly with a photochronograph at a scanning rate of 6 km/sec.

RESULTS

Shock-compression parameters were measured in several series of tests. For each series the same screen material was used and the shock wave produced in it had the same intensity. The results are given in Table I. This table lists the screen material and the pressure P_{sc} produced in it, the initial porosities m and the experimental values of the shock-wave velocity (D), as well as the other shock-compression parameters determined graphically in $P-U$ diagrams: the mass velocity behind the shock front (U), the pressure $P = \rho_0 UD/m$, the degree of compression $m\sigma = \rho/\rho_{00} = D/(D - U)$, and the density obtained by shock compression, expressed as the ratio of the final density to the bulk density, $\sigma = \rho/\rho_0$. The final column of Table I gives the number of experiments from which the average value of D was obtained. Accurate data on the dynamic compressibility of the screen materials [5] were used in the construction of the graphs. The data of Table I are represented by black dots in the $P-\sigma$ plot in Fig. 3.

Table I

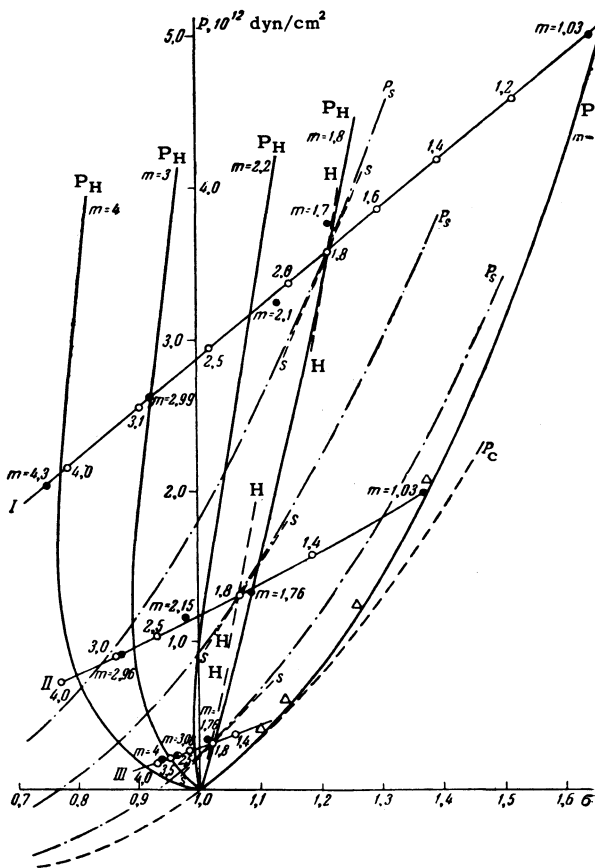| Test series	Screen material and P_{sc}, in 10^{12} dyn/cm^2	m	D, km/sec	U, km/sec	P, in 10^{12} dyn/cm^2	$m\sigma$	σ	No. of tests
I	iron 3.585	1.03	8.11	3.26	5.01	1.673	1.635	3
		1.70	8.02	4.12	3.76	2.058	1.211	5
		2.11	7.80	4.53	3.24	2.385	1.131	3
		2.99	7.95	5.09	2.62	2.775	0.928	5
		4.3	8.11	5.63	2.05	3.264	0.759	1
II	iron 1.39	1.03	6.01	1.74	1.98	1.406	1.365	2
		1.76	5.01	2.39	1.32	1.912	1.086	5
		2.15	4.96	2.60	1.16	2.102	0.978	4
		2.96	4.78	2.93	0.91	2.577	0.871	4
III	aluminum 0.258	1.76	2.56	1.12	0.315	1.778	1.011	10
		3.06	2.29	1.51	0.219	2.936	0.960	13
		3.99	2.28	1.67	0.185	3.726	0.934	3

FIG. 3. Shock adiabats of porous tungsten: ●—experimental points; ○—calculated data; △—results taken from[6].

To smooth out the experimental results and to permit interpolation, Fig. 3 has lines denoted by I, II and III, which represent approximately the data from three series of tests. Each point on one of these lines represents its intersection with a shock adiabat corresponding to some fixed initial porosity m.* The value of the porosity is related

*This follows from the equations of conservation of momentum and mass for tungsten, the equation giving the change of state of the screen material in P—U coordinates, and the equality of pressures and velocities at the boundary between the sample and the screen.

to the shock-compression parameters by

$$m = \sigma^{-1} + \rho_0 U^2/P.$$

The values of m are given in Fig. 3 next to the black dots.

Figure 4 gives the dependence of $(E - E_0)$ on σ along lines I, II, and III of Fig. 3. The quantity $E - E_0 = (P/2\rho_0)(m\sigma - 1)/\sigma$ represents the change of the total internal energy per unit mass of a porous sample subjected to shock compression (it is worth noting that $E - E_0 = U^2/2$). We shall use the smoothened results in our subsequent discussion.

Figure 3 shows also the shock adiabat of nonporous tungsten (m = 1). The points on this adiabat were obtained by short-range extrapolation and lie somewhat to the right of the points representing m = 1.03. Using Bridgman's data for the adiabat of nonporous tungsten, we put $D = D_0 + \lambda U$, where $D_0 = 4$ km/sec and $\lambda = 1285$. The triangles in Fig. 3 represent the results of[6] for samples with m = 1.01, these results agree with our data.

Thus, for each shock adiabat of tungsten corresponding to some initial porosity, we know three experimental points lying on lines I, II and III; the point P = 0, σ = 1 is common to all the adiabats.

For tungsten with m = 1.8, three series of sound-velocity measurements were carried out behond shock fronts. The results are given in Table II. The screen materials and the wave intensities in them were the same as in the corresponding series of tests listed in Table I. The lateral-relaxation angle α was found experimentally. The sound velocity was calculated from*

$$C = D \ [\text{tg}^2\alpha + (m\sigma)^{-2}]^{1/2}.$$

The sound velocity $C_1 = 6.1$ km/sec, calculated from the experimental value of α for the lower

*tg = tan

Table II

Test series	m	α deg	P, in 10^{12} dyn/cm^2	σ	D, km/sec	C, km/sec	dP/dσ 10^{12} dyn/cm^2	No. of tests
I	1.80	38.5	3.58	1.212	7.84	7.19	10.00	4
II	1.80	44.5	1.31	1.065	5.04	5.61	6.09	4
III	1.80	67	0.31	1.017	2.52	$C_1=6.1;\ C_2=4.79$	4.44	17

range of pressures, is very large. This value is greater than the 5.61 km/sec obtained for medium pressures, although in the latter case both the density and the pressure were higher. There is a reason for this inconsistency. Al'tshuler et al [4] have shown that in metals the angle α found experimentally at low pressures represents the velocity of an elastic wave which is $\nu = [3(1-\mu)/(1+\mu)]^{1/2}$ times greater than the velocity of waves of volume plastic deformation, which is the velocity we need. Assuming that in the lower range of pressures Poisson's ratio of tungsten is the same ($\mu = 0.3$) as at normal temperature and pressure*, we find that the sound velocity is $C_2 = 4.79$ km/sec; we shall use this value henceforth.

The experimental slopes of the isentropic curves, $(\partial P/\partial\sigma)_S = \rho_0 C^2$, are given in Fig. 3 by straight-line segments denoted by S.

DISCUSSION

1. The experimental results (Fig. 3) show that the Hugoniot adiabat of nonporous tungsten has its usual form: with increase of pressure the density of the shock-compressed metal rises and, therefore, the derivative $(dP/d\sigma)_H$, is positive everywhere along the adiabat. As the initial porosity of the material increases the shock compressibility falls rapidly and the corresponding adiabats are shifted toward smaller values of σ. For moderate porosities, e.g., $m < 2$, the adiabats still have the usual form: $\sigma > 0$, $(dP/d\sigma)_H > 0$. At higher porosities the density of shock-compressed tungsten ($\sigma < 1$) does not reach the density of nonporous metal at normal temperature and pressure. The initial portions of the adiabats for large values of m are unusual: for a given value of m the density decreases with increase of pressure and consequently $(dP/d\sigma)_H < 0$. These results are in qualitative agreement with the theory of the behavior of porous metals, given in the introduction.

There is, however, an important disagreement between the theory and experiment. The experimental results (Fig. 3) show that the shock adiabat

*The lower experimental point corresponds to a relatively low temperature, lower than the melting point at atmospheric pressure.

for a large value of m, e.g., m = 3, has the following form. It begins at P = 0, $\sigma = 1$ and first it deviates to the left into the region where $\sigma < 1$ and where the density decreases with increase of pressure, i.e., $(dP/d\sigma)_H < 0$. On further increase of pressure the density passes through a minimum value, $\sigma_{min} < 1$, at some finite point where $(dP/d\sigma)_H = \infty$, and then the density begins to rise. Thus there is a region where the derivative $(dP/d\sigma)_H$ is positive as for the usual adiabats. For this type of Hugoniot adiabats there are two points at different pressures where the density is the same (within the range $\sigma_{min} \leq \sigma \leq 1$). At a given density the point at higher pressure represents greater heating due to shock compression.

This behavior indicates that γ decreases strongly with increase of temperature. This decrease is due to increase of the specific heat of the metal with increase of temperature, mainly due to the greater contribution of the electrons to the specific heat at high temperatures. At T = 0 the coefficient γ is equal to the Grüneisen constant of the crystal lattice (γ_{lat}).

2. From the experimental results we can find the relationship between the thermal components of pressure, $P_T = P - P_c$, and of the internal energy, $E_T = E - E_c$, where

$$E_c = E_0 + \int_1^\sigma \frac{P_c}{\rho_0 \sigma^2}\, d\sigma;$$

where we confine ourselves to the results for very porous samples, i.e., we shall consider the region of high temperatures and a relatively narrow range of density changes ($0.75 < \sigma < 1.30$). The function $P_c(\sigma)$, i.e., the dependence of pressure on density at zero temperature (the difference between 0°K and ≈ 300°K can be neglected), is given by the following formula [7]

$$P_c = k_1\sigma^{4/3}\exp\left(-b/\sigma^{1/3}\right) - k_2\sigma^{4/3}, \qquad (1)$$

where $k_1 = 99.46 \times 10^{13}$ dyn/cm^2, $k_2 = 227.6 \times 10^{10}$ dyn/cm^2, and b = 6.08 were found from the experimental values of the density ρ_0, the bulk modulus, $-v_0 dP/dv = \rho_0 C_0^2$, and the lattice Grüneisen constant for normal conditions, $\gamma_{lat}^0 = 1.6$. The values of k_1, k_2, and b were calculated using the expression found by Dugdale and MacDonald (see, for example, [5]).
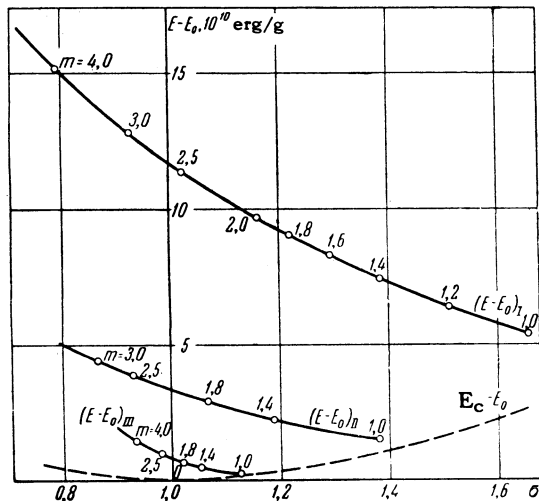
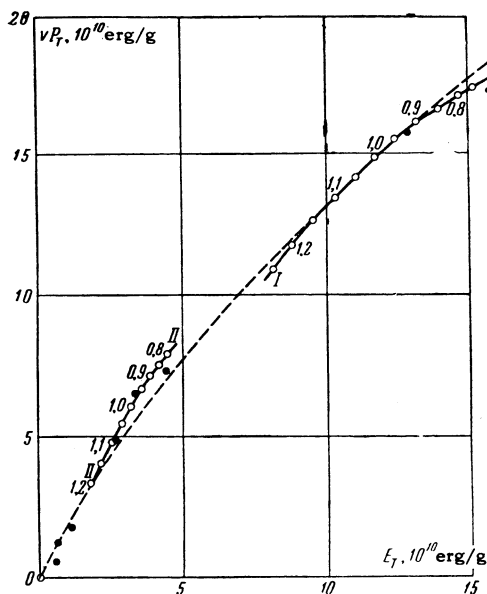FIG. 4. Dependences of $(E - E_0)$ on σ along lines I, II, III of Fig. 3.

FIG. 5. The vP_T-E_T diagram: ●— experimental points; o — calculated data.

Figure 5 gives the experimental results (black dots) and the lines I, II taken from Figs. 3 and 4, in coordinates of vP_T and E_T; the numbers represent the values of σ.

The ratio of the thermal pressure to the volume density of the thermal energy vP_T/E_T at any point is given directly by the slope of the straight line joining the origin of coordinates with that point. With increase of the thermal energy the ratio decreases. The positions of the points, denoted by open circles, for three ranges of pressures and at the same density σ lead to the following conclusions.

The relationship between the thermal components of the pressure and the internal energy is

nonlinear. The quantity γ, determined by the first derivative of vP_T with respect to E_T, decreases with increase of the thermal energy and, consequently, with increase of temperature. The second derivative of vP_T with respect to E_T is negative, i.e., $v(\partial^2 P/\partial E^2)_v < 0$. This and the thermodynamic equilibrium

$$\left(\frac{\partial C_v}{\partial T}\right)_S = - \frac{C_v^2}{\gamma} \left(\frac{\partial^2 P}{\partial E^2}\right)_v$$

show that along an isentropic curve the specific heat of the metal, $C_V = (\partial E/\partial T)_V$, rises with temperature.

To obtain a clearer picture of the shock adiabats we shall use the fact that in the first (rough) approximation the experimental data for various values of σ can be described by a unique dependence of E_T on vP_T. The simplest form of this dependence is

$$E_T = a (vP_T) + b (vP_T)^2 \qquad (2)$$

where $a = 0.5$ and $b = 1.99 \times 10^{-12}$ g/dyn-cm. The plot of this dependence is the dashed curve in Fig. 5. Selection of this particular dependence is equivalent to the assumption that the quantity $\gamma_{lat} = 1/a$ is constant in the range of densities considered.

Equation (2), together with Eq. (1), can be regarded as the empirical equation of state, relating P, E and v [the equation of state in the form $P_T = BT/v$, $E_T = C_VT + \beta T^2/2$ can be reduced to Eq. (2)]. Using the empirical equation of state we can now determine the behavior of both the shock and isentropic adiabats, but we cannot use this equation for long-range extrapolation. The shock adiabats P_H calculated using Eq. (2) with m = 1.8, 2.2, 3, and 4 and the isentropic curves P_S are given in Fig. 3. The calculated shock adiabats lie near the points defined by the experimental lines I, II, and III.

3. The experimental results give a system of intersecting curves in P—σ coordinates: these are segments of isentropic curves cut by the lines I, II, and III. Hence the value of γ and the slopes of the shock adiabats can be found independently, using the expression

$$\frac{dE}{dv} = \left(\frac{\partial E}{\partial P}\right)_v \frac{dP}{dv} + \left(\frac{\partial E}{\partial v}\right)_P \qquad (3)$$

for the total derivative of the internal energy with respect to volume. If the values of dE/dv and dP/dv are known for two lines at their intersection point, we can find the partial derivatives $(\partial E/\partial P)_v$ and $(\partial E/\partial v)_P$. The first of these partial derivatives gives the important thermodynamic parameter γ.

Table III

Hugoniot adiabat points (m = 1.8)		$(\partial E/\partial v)_P$, 10^{10} erg/cm^3	$(\partial E/\partial P)_v$, cm^3/g	$\gamma = v\,(\partial P/\partial E)_v$	$(dP/d\sigma)_H$, 10^{10} dyn/cm^2
P, 10^{12} dyn/cm^2	σ				
3.58	1.212	677	0.036	1.17	2430
1.31	1.065	264	0.025	1.64	2130
0.31	1.017	210	0.027	1.87	1840

Let us illustrate this by considering a particular case. From our experiments we know for each of three points on the shock adiabat with m = 1.8 the total derivatives along two lines: along the isentropic curve, where $(dE/dv)_S = -P$ and $(dP/dv)_S = -(\rho_0 \sigma C)^2$ is given by the measured velocity of sound (Table II), and along line I (or II, or III), where the derivatives dP/dv and dE/dv are found from graphs in Figs. 3 and 4. The values of γ and $(\partial E/\partial v)_P$ found for the three points on the shock adiabat with m = 1.8 are listed in Table III.

For the Hugoniot adiabat with m = 1.8 the quantity γ varies from the range 1.54—1.70* (at the point P = 0, $\sigma = 1$) to 1.17 at the highest pressures reached in the tests. This drop in γ is primarily due to the increase in temperature. It is difficult to see why γ is greater than γ^0_{lat} at lower pressures; this may possibly be due to experimental errors.

We shall now substitute the partial derivatives and the relationship

$$(dE/dv)_H = \tfrac{1}{2}[(mv_0 - v)(dP/dv)_H - P]$$

for the Hugoniot adiabat into an equation such as Eq. (3). Solving this equation for $(dP/dv)_H$, we find the slopes of the shock adiabats listed in Table III. In Fig. 3 these slopes are marked by the letter H.

4. The behavior of the shock adiabat depends strongly on the quantity γ. By examining the general relationship between $(dP/d\sigma)_H$ and γ we can find by still another method the limits of variation of γ, and sometimes also its magnitude. Let us write down the expression for the Hugoniot adiabat in its differential form:

$$-j^2\left(\frac{dv}{dP}\right)_H = \frac{M^2(1-z)}{1-M^2 z}, \qquad (4)$$

$$j = \rho_{00}D = \frac{\rho_0}{m}D, \quad M = \frac{\rho_{00}D}{\rho C} = \frac{D-U}{C}, \quad z = \frac{1}{2}\gamma(m\sigma - 1).$$
Here
$$(5)$$

$$-\left(\frac{dv}{dP}\right)_H = \frac{1}{\rho_0 \sigma^2}\left(\frac{d\sigma}{dP}\right)_H$$

is the derivative of the Hugoniot adiabat. The de-

nominator in Eq. (4) is always positive in those regions of the adiabat where the shock wave is stable. This follows from the condition $0 \le M < 1$ (see, for example, [8]) and from the inequality on the left-hand side of the following criterion of stability, derived by D'yakov: [9]

$$-1 < j^2(dv/dP)_H < 1 + 2M. \qquad (6)$$

If the inequality on the right-hand side of Eq. (6) is used as well, then the denominator in Eq. (4) is subject to a more restrictive condition:

$$(1 - M^2 z) > \tfrac{1}{2}(1 - M) > 0.$$

Thus the sign of $-(dv/dP)_H$ is governed by the sign of the numerator, i.e., by the sign of $(1 - z)$.

It follows that along those segments of the adiabat where $(dP/d\sigma)_H > 0$, the inequality $\gamma < 2/(m\sigma - 1)$ should be satisfied; along the segments where $(dP/d\sigma)_H < 0$, the quantity γ is given by

$$\frac{1+M}{2M^2}\frac{2}{m\sigma-1} > \gamma > \frac{2}{m\sigma-1};$$

in the segments where $dP/d\sigma = \infty$ we have $\gamma = 2/(m\sigma - 1)$.

We can conclude for the foregoing, for example, that for the highest experimental point of the adiabat with m = 3 [the point on line I in Fig. 3 where $(dP/d\sigma)_H > 0$] we have

$$\gamma < 2/(3 \cdot 0.922 - 1) = 1.13,$$

i.e., the value of γ is considerably smaller than the Grüneisen constant under normal conditions.

It is of interest to consider in detail the segments of the shock adiabats where the density has an extremum. We have not studied these segments in detail, but for m = 3 the density minimum can be taken as the point in the medium range of pressures (line II in Fig. 3). At this point we find

$$\gamma = 2/(3 \cdot 0.865 - 1) = 1.26;$$

the value of γ decreases along the adiabat above this point, and rises below it.

When a porous body is compressed by a wave with an infinitesimally small amplitude (P → 0, σ → 1, D → 0, U → 0, C → C$_0$) we obtain from (4) the result, reported by E. I. Zababakhin, that at the point P = 0, $\sigma = 1$

---

*This range contains the values of the Grüneisen constant γ^0_{lat} for normal conditions, as reported by various workers.

$(dP/d\sigma)_H > 0$ when $m < (1 + 2/\gamma_{lat}^0)$,

$(dP/d\sigma)_H = \infty$ when $m = (1 + 2/\gamma_{lat}^0)$,

$(dP/d\sigma)_H < 0$ when $m > (1 + 2/\gamma_{lat}^0)$.

5. It is interesting to consider qualitatively the shock adiabats at pressures much greater than those reached in our experiments. Figure 6 gives the experimental Hugoniot adiabats and the adiabats constructed using the Thomas-Fermi model (TF) and Latter's data.[10] If the experimental curves have density minima, then the TF shock adiabats have density maxima above which the density falls with increase of pressure, approaching gradually a value representing a fourfold compression. The TF adiabats at the density maxima have values of $\gamma = 2/(m\sigma_{max} - 1)$ varying from about 0.48 to 0.39 when m changes from 1 to 4. Above the density maxima, the value of γ rises, approaching $2/3$ as $P \to \infty$.
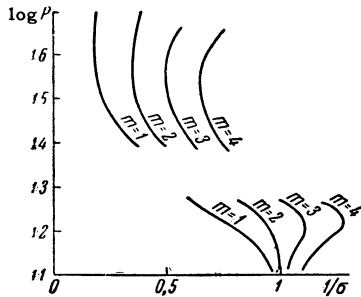

FIG. 6. Extrapolation of dynamic adiabats.

Thus the shock adiabats of a metal can have various forms with positive and negative slopes; in particular, the adiabats can be S-shaped at large values of m. D'yakov[9] showed that such adiabats can have segments where the shock waves are unstable. Our analysis of the stability criteria showed no such segments either in the TF adiabats or in the experimental adiabats, calculated from the equation of state (2). Moreover, no segments were found where a shock front can generate sound spontaneously, though such generation was predicted by D'yakov.

6. Let us now estimate the temperatures reached in shock compression of porous tungsten. We shall take the heat capacity as $C_V = C_{V0} + \beta T$, where the first term is the lattice specific heat according to Dulong and Petit, and the second term gives the contribution of the electrons. The coefficient $\beta = 1.11 \times 10^{-3}$ J/mole-deg was taken from the data of Waite et al,[11] who carried out measurements close to the absolute zero. The temperatures were calculated using

$$E_T = \int_0^T C_v dT.$$

Table IV lists the calculated temperatures for two

Table IV

Point on adiabat	Characteristic point		E_T, 10^{10} erg/g	T, 10^3 deg K
	P, 10^{12} dyn/cm^2	σ		
$m = 1.8$ {	3.58	1.212	8.682	21.6
	1.31	1.065	2.875	4.11
	0.31	1.017	0.648	2.27
$m = 2.59$	2.865	1	11.77	27.1
$m = 2.096$	1.174	1	3.32	10.0
$m = 2.06$	0.285	1	0.78	2.7
$m = 4$ {	2.160	0.789	14.87	32.0
	0.727	0.773	4.64	13.2
	0.187	0.938	1.38	4.73

Hugoniot adiabats with m = 1.8 and m = 4 (three experimental points for each) and for a density $\sigma = 1$ equal to the initial density of nonporous tungsten (also three experimental points). The calculations were carried out for the points lying on lines I, II, and III (Fig. 3).

[1] Ya. B. Zel'dovich, JETP 32, 1577 (1957), Soviet Phys. JETP 5, 1103 (1957).

[2] Al'tshuler, Krupnikov, Ledenev, Zhuchikhin, and Brazhnik, JETP 34, 874 (1958), Soviet Phys. JETP 7, 606 (1958).

[3] Al'tshuler, Krupnikov, and Brazhnik, JETP 34, 886 (1958), Soviet Phys. JETP 7, 614 (1958).

[4] Al'tshuler, Kormer, Brazhnik, Vladimirov, Speranskaya, and Funtikov, JETP 38, 1061 (1960), Soviet Phys. JETP 11, 766 (1960).

[5] Al'tshuler, Kormer, Bakanova, and Trunin, JETP 38, 790 (1960), Soviet Phys. JETP 11, 573 (1960).

[6] R. G. McQueen and S. P. Marsh, J. Appl. Phys. 31, 1253 (1960).

[7] B. I. Davydov, Izv. AN SSSR, ser. geofiz. 12, 1441 (1956).

[8] L. D. Landau and E. M. Lifshitz, Mekhanika sploshnykh sred. (Mechanics of Continuous Media) Gostekhizdat, 1954.

[9] S. P. D'yakov, JETP 27, 288 (1954); V. M. Kontorovich, JETP 33, 1525 (1957), Soviet Phys. JETP 6, 1179 (1958).

[10] R. Latter, Phys. Rev. 99, 1854 (1955).

[11] Waite, Craig, and Wallace, Phys. Rev. 104, 1240 (1956).